

Anisotropic characteristics analysis of 3D-printed optics

Tobias Grabe* **, Tobias Biermann* ***, Maximilian Bayerl*, Roland Lachmayer* ** **

*Institute of Product Development, Leibniz University Hannover, D-30823 Garbsen

**GROTESK, D-30167 Hannover

***Cluster of Excellence PhoenixD, D-30167 Hannover

mailto:grabe@ipeg.uni-hannover.de

The Additive Manufacturing of transparent materials enables cost efficient rapid prototyping of optically transparent components. The components are built layer-by-layer which can cause anisotropic optical properties. We present the quantitative analysis of anisotropic imaging and its dependence on the layer thickness of MJM-printed transparent samples.

1 Introduction

For the design of optical transparent elements, Additive Manufacturing offers a great potential to produce cost efficient individually adapted freeform optics [1][2]. One of the most common and commercially available printing processes for transparent polymers is Multi-Jet Modeling (MJM) [3]. During the layer-by-layer curing of the material, its optical properties are changed. Thus, the optically scattering effects in the materials volume can be identified [4]. Without quantification of these properties, the design quality of Additive Manufactured optics in products is limited [5]. In this work, the impact of the layer thickness on the optical volume scattering of MJM-manufactured parts will be quantitatively evaluated.

2 Multi-Jet Modeling

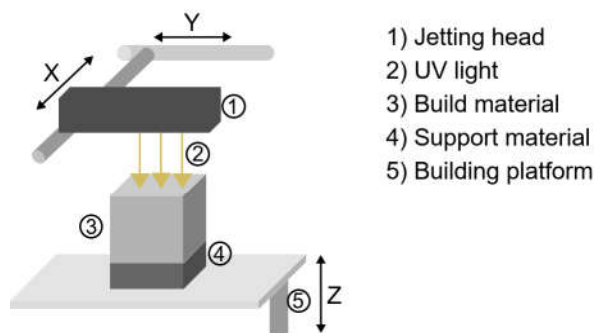


Fig. 1 Multi-Jet Modeling setup

The samples were manufactured on an Objet30 Pro. In MJM the print heads are applying a photopolymer drop-by-drop on a platform, which are cured by UV light (Fig. 1). For printing, the resin VeroClear is used. In the horizontal plane the printing resolution is 600 dpi.

3 Experimental Set-up

Equilateral cubes with an edge length of 25 mm are printed with 16 μm and 32 μm layer thickness

and all planes are polished. For the analysis a laser beam is propagating through a cube perpendicular to the plane in X-, Y- and Z-axis orientation. The orientations are defined in Fig. 1. The beam is projected on a surface at 143 mm distance to the cube and is detected by a CMOS sensor. For the measurement a Helium-Neon laser with a wavelength of $\lambda = 632 \text{ nm}$ at a maximum power of 1 mW, a Gaussian power distribution and a collimation beam diameter of 2 mm is used.

4 Results

The projected beam profile which results of the laser beam propagating through the sample from different directions is shown in Fig. 2 for a layer thickness of 16 μm . Here, the anisotropic optical properties of the transparent polymer samples are visible. For quantitative analysis, the coordinate central point is defined at the maximum intensity of the scattered light.

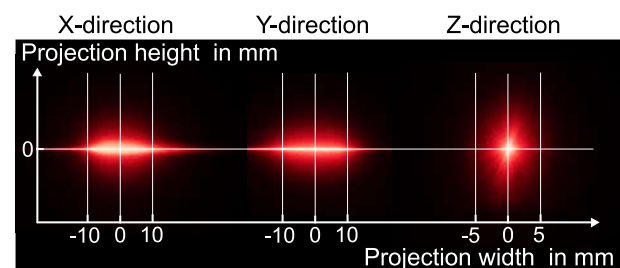


Fig. 2 Scattering patterns on the projection surface.

The intensity matrix I shown in Eq. 1 is derived from the sensor data where $i_{h,w}$ denotes the brightness value of a pixel on the sensor. Here, h denotes the vertical position and w the horizontal position of the pixels on the sensor array. The evaluation for the vertical axis is explained exemplary. The normalized energy $f_I(h)$ along the horizontal axis is calculated by the sum of the vertical matrix entries according to Eq. 2.

$$\mathbf{I} = i_{h,w} = \begin{pmatrix} i_{1,1} & \cdots & i_{1,m} \\ \cdots & \cdots & \cdots \\ i_{n,1} & \cdots & i_{n,m} \end{pmatrix} \quad (1)$$

$$f_I(h) = \sum_{w=1}^m i_{h,w} \quad (2)$$

The measurement results for the vertical (h) and horizontal (w) matrix analysis for laser beam crossing a cube with 16 μm and 32 μm layer thickness in X-, Y- and Z-direction are shown in Fig. 3 and Fig. 4. Here, the results for $f_I(w)$ are normalized to the global maximum value of all measurements.

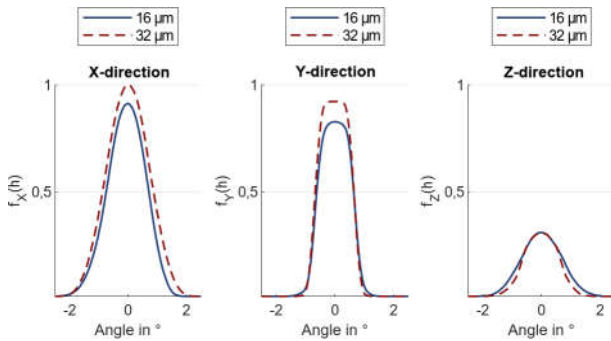


Fig. 3 Normalized intensity profile (projection height)

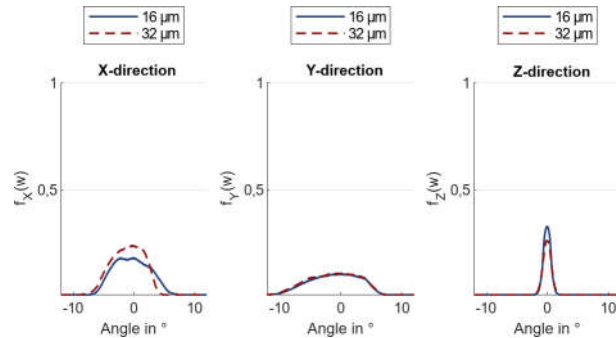


Fig. 4 Normalized intensity profile (projection width)

When the laser beam is crossing the sample in X-direction for $f_x(h = 0)$ a value of 1 and $f_x(w = 0) = 0.23$ is detected for a layer thickness of 32 μm . For a layer thickness of 16 μm a value of $f_x(h = 0) = 0.91$ and $f_x(w = 0) = 0.17$ is determined. A scattering cone angle of approximately 2° for vertical scattering and 5° for horizontal scattering can be detected. In Y-direction, a maximum of $f_y(h = 0) = 0.92$ and $f_y(w = 0) = 0.10$ for a layer thickness of 32 μm and maximum of $f_y(h = 0) = 0.83$ and also $f_y(w = 0) = 0.10$ is determined for a layer thickness of 16 μm . Here, a smaller scattering cone angle of approximately 1° for vertical scattering and 8° for a non-symmetric horizontal scattering can be detected. In Z-direction a maximum of $f_z(h = 0) = 0.30$ for the two analyzed layer thicknesses is detected. Further, $f_z(w = 0) = 0.32$

for 16 μm and $f_z(w = 0) = 0.25$ for 32 μm layer thickness is determined. The doubled layer thickness leads to a decreasing of the vertical scattering cone angle from 2° to 1.5° while the horizontal cone angle remains stable with 1.5° .

5 Discussion and Outlook

In this paper, an initial analysis of the impact of the layer thickness on the optical volume scattering of MJM-manufactured parts is performed. The optical scattering of transparent MJM-printed parts depends on the sample's orientation during the manufacturing process. When the laser beam is crossing the sample in X- and Y-direction, a line-shaped scattering pattern occurs. The normalized energy which is transmitted through the sample along these directions is significantly increased when a larger layer thickness is used for sample manufacturing. However, in Z-direction an increased layer thickness shows a minor decrease of the normalized energy.

By transferring these results into a simulation, MJM-printed optical components can be used to selectively utilize these properties for the use in optical products. Thus, potentially the use of MJM-printed parts for novel, tailored designed optical components can be improved majorly.

6 Acknowledgment

The research was conducted within the framework of the project "GROTESK-Generative Fertigung optischer, thermaler und struktureller Komponenten" funded by EFRE-NBank (ZW6-85018307) and by the Deutsche Forschungsgemeinschaft (DFG, German Research Foundation) in Germany's Excellence Strategy within the Cluster of Excellence PhoenixD (EXC 2122, Project ID 390833453).

References

- [1] T. Grabe, Y. Li, H. Krauss, A. G. Wolf, J. Wu, C. Yao, Q. Wang, R. Lachmayer, and W. Ren, "Freeform optics design for Raman spectroscopy," in *Photonic Instrumentation Engineering VII*, Y. Soskind and L. E. Busse, eds. (SPIE, 2020).
- [2] R. Lachmayer, R. B. Lippert, and S. Kaielerle, *Konstruktion für die Additive Fertigung 2018* (Springer Berlin Heidelberg, Berlin, Heidelberg, 2020).
- [3] G. Leuteritz, R. B. Lippert, K. Rettschlag, and R. Lachmayer, "Comparison of Additive Manufacturing techniques regarding mechanical and optical properties," (DGaO, 2018).
- [4] M. Rank, A. Horsak, M. Kudlek, J. Nuding, S. Pekrul, and A. Heinrich, "Diffraktive Effekte an additiv gefertigten optischen Elementen," (DGaO, 2017).
- [5] M. Rank and A. Heinrich, *3D Printing of Optics*, vol. SL39 (SPIE, 2018).